

# The effect of under sea level on the transmission of signals for FBG

Khaled S. Fehaed

Faculty of Science, King Saud University, Riyadh and University of Tabuk, Saudi Arabia

**Abstract**— The transmission and the reflection of Fiber Bragg grating (FBG) are calculated theoretically under ocean. The nonlinear effects appear on the reflectivity and the transmittivity of traveling signals. A full study for the performance of the nine apodization profiles for the FBG under the effect of temperature, pressure and water depth are investigated. Then, schedules have been done for the optimum values for the reflectivity of all types, selecting the appropriate profile which is the Sinc one giving about 99% reflectivity for the grating.

**Keywords**— FBG, Transmission, Reflectivity.

## I. INTRODUCTION

An FBG is an optical fiber, in which the refractive index in a part of its core is perturbed forming a periodic or quasi-periodic index modulation profile. A narrow band of the incident optical field within the fiber is reflected by successive, coherent scattering from the index variations. When the reflection from a crest in the index modulation is in phase with the next one, we have maximum mode coupling or reflection. Then, the Bragg condition is fulfilled. By modulating the quasi-periodic index perturbation in amplitude and (or) phase, we may obtain different optical filter characteristics. The formation of permanent gratings by photosensitivity in an optical fiber was first demonstrated by Hill et al. in 1978 [1].

Because an FBG can be designed to have an almost arbitrary, complex reflection response, it has a variety of applications, well described by Hill and Meltz among others [2]. For telecommunications, the probably most promising applications have been dispersion compensation [3] and wavelength selective devices [4] depending on its reflectivity. Examples of the latter are filters for WDM systems [5].

Any change in the fiber properties, such as strain, temperature, or pressure which varies the modal index or grating pitch, will change the Bragg wavelength. Therefore, this change is studied in the following, including undersea fiber cables that use WDM techniques. Both linear and nonlinear fibers are taken into consideration.

## II. MATHEMATICAL MODEL

The refractive index along the grating length varies periodically in the form [6]

$$n(z) = n_0 + n_1(z) \cdot \cos\left[\frac{2\pi}{\Lambda} z + \phi(z)\right] + n_2 E^2(z), \quad (1)$$

where  $E(z)$  is the electric field,  $n_0$  is the average refractive index change of the fiber core,  $n_1(z)$  is the amplitude of periodic index change,  $n_2$  is the nonlinear Kerr coefficient,  $\Lambda$  is the Bragg period and  $\Phi(z)$  describes the phase shift.

The electric field inside the grating can be written as

$$E(z, t) = [A_f(z, t) \exp(ikz) + A_b(z, t) \exp(-ikz)] \exp(i\omega_0 t), \quad (2)$$

Where  $A_f$  and  $A_b$  are the envelope functions of the forward and backward traveling waves, both of which are assumed to be slowly varying in space and time,  $\omega_0$  is the carrier frequency at which the pulse spectrum is initially centered and  $k$  is the propagation constant.

To describe nonlinear pulse propagation in the FBG, one can use the nonlinear coupled mode equations that are valid only for wavelengths close to the Bragg wavelength,  $\lambda_B$ . The nonlinear coupled mode equations take the form [6]

$$i \frac{dA_f}{dz} + \frac{i}{v_g} \frac{dA_f}{dt} + \delta A_f + \kappa A_b + \gamma(|A_f|^2 + 2|A_b|^2) A_f = 0, \quad (3)$$

and

$$-i \frac{dA_b}{dz} + \frac{i}{v_g} \frac{dA_b}{dt} + \delta A_b + \kappa A_f + \gamma(|A_b|^2 + 2|A_f|^2)A_b = 0, \quad (4)$$

where  $v_g$  is the group velocity far from the stop band associated with the grating,  $\gamma$  is called the nonlinear term and can be calculated from [6]

$$\gamma = \frac{2\pi}{\lambda_B} n_2. \quad (5)$$

The term  $\kappa$  is called the linear coupling coefficient and is defined by

$$k(z) = \frac{\pi n_1(z)}{\lambda_B} \exp(i\phi(z)). \quad (6)$$

To solve Eqs.(3) and (4), one neglects the time derivative term and assume the following forms for the solutions

$$A_f = u_f \exp(iqz) \text{ and } A_b = u_b \exp(iqz), \quad (7)$$

Where  $u_f$  and  $u_b$  are constants along the grating length. By introducing a parameter  $f=u_b/u_f$  that describes how the total power  $P$  is divided between the forward and the backward propagating waves, the power can be calculated as

$$u_f^2 + u_b^2 = P_o. \quad (8)$$

Both  $q$  and  $\delta$  are found to depend on  $f$  and are given by [6]

$$q = -\frac{k(1-f^2)}{2f} - \frac{\gamma P_o}{2} \frac{1-f^2}{1+f^2}, \quad (9)$$

$$\delta = -\frac{k(1+f^2)}{2f} - \frac{3\gamma P_o}{2}, \quad (10)$$

In general, the nonlinear coupled mode equations should be solved numerically for studying the nonlinear effects. Using the fourth order RungeKutta method, Eqs. (3) and (4) are solved, in which the values of  $A_f$ ,  $A_b$  can be obtained exactly along the grating length and then the new values of the refractive index are calculated.

Using the coupled mode theory of Lam and Garside that describes the reflection properties of the FBG, the reflectivity of a grating with constant modulation amplitude is given by [3]

$$R(l, \lambda) = \frac{\Omega^2 \sinh^2(sl)}{\Delta k \sinh^2(sl) + s^2 \cosh^2(sl)} \quad (11)$$

where  $R(l, \lambda)$  is the reflectivity that is a function of the grating length,  $l$  and wavelength,  $\lambda$ .  $\Delta k = k - \pi / \lambda$  is the detuning wave vector, and  $s^2 = \Omega^2 - \Delta k^2$ .

The coupling coefficient,  $\Omega$ , for sinusoidal variation of index perturbation along the fiber axis is given by [3]

$$\Omega = \frac{\pi \Delta n}{\lambda} M_p \quad (12)$$

where  $M_p$  is the fraction of the fiber mode power contained by the fiber core. On the basis that the grating is uniformly written through the core,  $M_p$  can be calculated by

$$M_p = 1 - V^{-2} = 1 - \left[ \left( \frac{2\pi}{\lambda} \right) a (n_{co}^2 - n_{cl}^2)^{1/2} \right]^{-2} \quad (13)$$

where  $V$  is the normalized frequency of the fiber,  $a$  is the core radius,  $n_{co}$ ,  $n_{cl}$  are respectively, the core and cladding indices. At the Bragg center wavelength, there is no detuning wave vector and  $\Delta k = 0$ . Therefore, the expression for the reflectivity becomes

$$R(l, \lambda) = \tanh^2(\Omega l) \quad (14)$$

The reflectivity increases with the induced index of refraction change. Similarly, as the length of the grating increases so does the resultant reflectivity.

Also, one can calculate the transmissivity of the waves through the FBG from [4]

$$T = \left[ \frac{4\delta^2 k^2 \sinh^4 \left[ (k^2 - \delta^2)^{1/2} \frac{l}{2} \right]}{(k^2 - \delta^2)^2} + 1 \right]^{-1} \quad (15)$$

So, one can study the effect of the FBG nonlinearity by measuring the reflectivity and the transmissivity of the signal moving in the grating.

The main apodization profiles considered in the present investigation are [7 and 8]

### 2.1 Sine profile

$$f(z) = \sin^2 \left( \frac{\pi z}{L} \right), \quad 0 \leq z \leq L \quad (16)$$

### 2.2 Sinc profile

$$f(x) = \frac{\sin(x)}{x}, \quad x = \frac{2\pi(z - \frac{L}{2})}{L}, \quad 0 \leq z \leq L \quad (17)$$

### 2.3 Positive-Tanh profile

$$f(x) = \tanh \left[ \frac{2az}{L} \right], \quad 0 \leq z \leq \frac{L}{2}$$

$$= \tanh \left[ \frac{2a(L-z)}{L} \right], \quad \frac{L}{2} \leq z \leq L \quad (18)$$

### 2.4 Blackman profile

$$f(z) = \frac{1 + 1.19 \cos(x) + 0.19 \cos(2x)}{2.38}, \quad x = \frac{2\pi(z - \frac{L}{2})}{L}, \quad 0 \leq z \leq L \quad (19)$$

### 2.5 Gauss profile

$$f(x) = \exp \left[ -G \left( \frac{z}{L} \right)^2 \right], \quad 0 \leq z \leq L \quad (20)$$

### 2.6 Hamming profile

$$f(x) = \frac{1 + H \cos\left(\frac{2\pi z}{L}\right)}{1 + H}, \quad 0 \leq z \leq L \quad (21)$$

### 2.7 Cauchy profile

$$f(x) = \frac{1 - \left(\frac{2z}{L}\right)^2}{1 - \left(\frac{2Cz}{L}\right)^2}, \quad 0 \leq z \leq L \quad (22)$$

### 2.8 Bartlett profile

$$\begin{aligned} f(x) &= \Delta n \left[ \frac{2z}{L} \right], \quad 0 \leq z \leq \frac{L}{2} \\ &= \Delta n \left[ -2\left(\frac{z}{L} - 1\right) \right], \quad \frac{L}{2} \leq z \leq L \end{aligned} \quad (23)$$

### 2.9 Raised sine profile

$$f(x) = \sin^2 \left[ \frac{\pi z}{L} \right], \quad 0 \leq z \leq L \quad (24)$$

## III. RESULTS AND DISCUSSION

### 3.1 Temperature Effect

Figure 1 shows the variation of the reflectivity with the wavelength of the signal traveling in the chirped FBG in the linear and nonlinear cases for the Sine profile. The variations of the reflectivity have been calculated under the effect of the temperature range 10 - 25°C. The increase that occurs in the values of the reflectivity due to the nonlinearity of the chirped grating enhances the performance of the FBG. This nonlinearity is explained by the perturbation of molecules when high power signals pass through the fiber

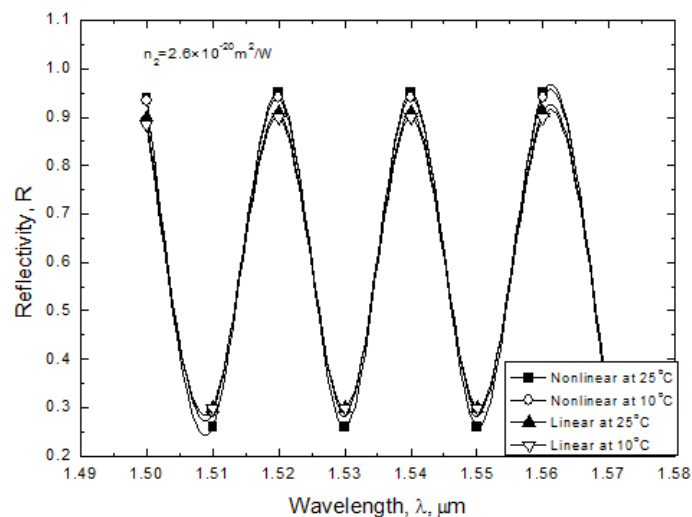


**FIG. 1 EFFECT OF THE TEMPERATURE ON THE REFLECTIVITY WITH WAVELENGTH IN THE LINEAR AND NONLINEAR CASES OF THE APODIZED CHIRPED GRATING (SINE PROFILE)**

The other apodization profiles will be similar and the corresponding optimum values are given in Table I. As shown in Table I, the **Sine** profile has the highest value of the reflectivity. It is considered the best profile for the selection of the wavelengths in all the chirped apodized grating profiles ( $R \approx 0.99$ ). The Blackman, Sine, Raised Sine, Gauss and Cauchy profiles are considered the second order of the wavelengths selection because of lower reflectivity ( $\approx 0.95$ ). The Tanh, Bartlett and

Hamming profiles have the lowest performance in the wavelengths selection (in the linear and nonlinear cases). All the profiles show a change in reflectivity ( $\approx 0.2$ ) when the temperature changes from  $25^{\circ}\text{C}$  to  $10^{\circ}\text{C}$ . This is the range of the change in temperature under the ocean depth. It is recommended to operate the FBG in the nonlinear region when the temperature decreases under the ocean depth.

**TABLE 1**  
**THE MAXIMUM VALUES OF REFLECTIVITY,  $R_{\max}$ , FOR THE DIFFERENT PROFILES IN THE LINEAR AND NONLINEAR CASES AT  $25^{\circ}\text{C}$  and  $10^{\circ}\text{C}$**

Profile	Linear Case $n_2 = 0 \text{ m}^2/\text{W}$		Nonlinear Case $n_2 = 2.6 \times 10^{-20} \text{ m}^2/\text{W}$	
	$R_{\max}$ at $25^{\circ}\text{C}$	$R_{\max}$ at $10^{\circ}\text{C}$	$R_{\max}$ at $25^{\circ}\text{C}$	$R_{\max}$ at $10^{\circ}\text{C}$
Blackman	0.92	0.91	0.96	0.95
Cauchy	0.91	0.9	0.95	0.94
Sinc	0.94	0.92	0.99	0.96
Sine	0.91	0.9	0.95	0.94
Tanh	0.88	0.87	0.91	0.89
Gauss	0.91	0.9	0.95	0.94
Hamming	0.85	0.84	0.88	0.87
Bartlett	0.89	0.88	0.915	0.89
Raised Sine	0.9	0.885	0.94	0.935

### 3.2 Pressure Effect

It is well known that the glass refractive index increases with pressure. This leads to increase the grating reflectivity. The variation of the reflectivity of the FBG with the wavelength of the signals propagating in the **Sine** profile through the linear and nonlinear chirped grating under the effect of pressure variation from 0 to 10MPa is displayed in Fig. 2.

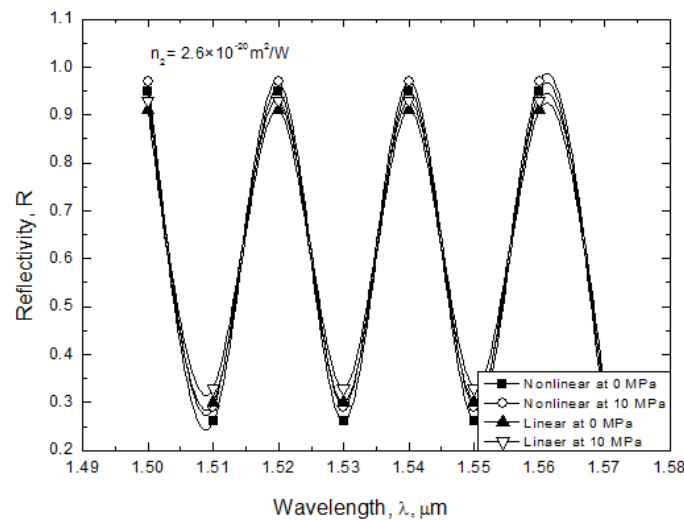


**FIG. 2 EFFECT OF THE PRESSURE ON THE REFLECTIVITY WITH WAVELENGTH IN THE LINEAR AND NONLINEAR CASES OF THE APODIZED CHIRPED GRATING (SINE PROFILE).**

The same procedure is repeated for the other apodization profiles and the optimum values of FBG reflectivity are summarized in Table II. As seen in Table II, the highest value of the reflectivity is the **Sinc** profile where its value in the nonlinear case reaches the maximum reflectivity ( $\approx 1$ ). So, it is considered the best profile for the selection of the wavelengths in all of the apodized profile. The Blackman, Sine, Raised Sine, Gauss and Cauchy profiles are considered in the second rank having lower values of reflectivity in the nonlinear case ( $\approx 0.95$ ). The Tanh, Bartlett and Hamming profiles

operate with lower performance in the wavelengths selection (in the linear and nonlinear cases) having the smallest values in the reflectivity ( $\approx 0.9$ ).

**TABLE 2**  
**THE MAXIMUM VALUES OF REFLECTIVITY,  $R_{\max}$ , FOR THE DIFFERENT PROFILES IN THE LINEAR AND NONLINEAR CASES AT 0 AND 10 MPa.**

Profile	Linear Case $n_2 = 0 \text{ m}^2/\text{W}$		Nonlinear Case $n_2 = 2.6 \times 10^{-20} \text{ m}^2/\text{W}$	
	$R_{\max}$ at 0 MPa	$R_{\max}$ at 10 MPa	$R_{\max}$ at 0 MPa	$R_{\max}$ at 10 MPa
Blackman	0.92	0.94	0.96	0.98
Cauchy	0.91	0.93	0.95	0.97
Sinc	0.94	0.96	0.99	1
Sine	0.91	0.93	0.95	0.97
Tanh	0.88	0.9	0.91	0.92
Gauss	0.9	0.92	0.93	0.95
Hamming	0.85	0.87	0.88	0.9
Bartlett	0.89	0.905	0.92	0.925
Raised sine	0.875	0.915	0.935	0.95

### 3.3 Water Depth Effect

The existence of any fiber cable under ocean depth acts to change the behavior of this cable, because of the temperature decrease and the pressure increase. One aims here to study the reflectivity of the apodized chirped Bragg grating under ocean depth. The Effect of the ocean depth on the reflectivity for the **Sine** apodization profile is shown in the Fig. 3. The ocean depth will change from 0 km and 1 km. The temperature variation, in this range will be from  $27^\circ\text{C}$  till  $8^\circ\text{C}$ . Also, the pressure is changed from 0 to 10 MPa. One can predict that the increase in the reflectivity that results from the pressure will approximately cancel the temperature effect.

Table III shows a comparison between the maximum reflectivity at the sea level and at 1 km ocean depth in the linear and nonlinear cases for all apodization profiles. It is clear that the reflectivity of 7 profiles increases with the ocean depth. This is because the pressure of 1 km depth (10 MPa) causes an increase in the reflectivity greater than the decrease in the reflectivity that result from the drop in the temperature at 1 km ( $8^\circ\text{C}$ ). In the **Sinc** profile, the change in pressure and in the temperature gives the same change in the reflectivity. So, the net change in the reflectivity will be zero. Finally, the Tanh profile has a decreased reflectivity because the decrease due to temperature is greater than the increase due to the pressure effect. So, the values of the reflectivity will decrease in the Tanh profile than that at the sea level

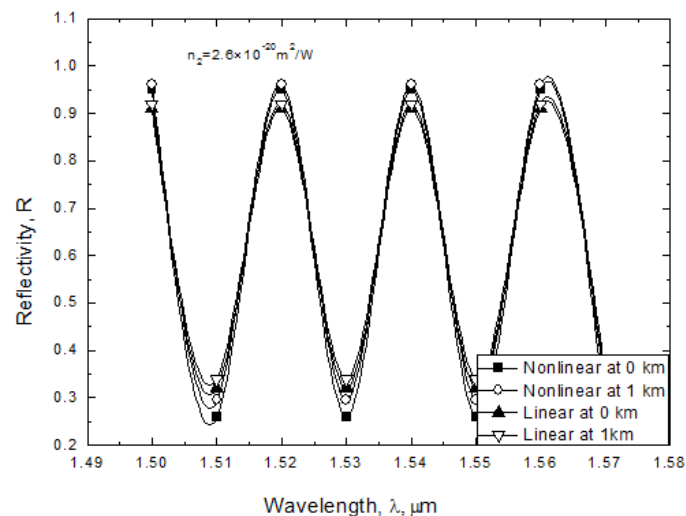


**FIG. 3 EFFECT OF THE OCEAN DEPTH ON THE REFLECTIVITY WITH WAVELENGTH IN THE LINEAR AND NONLINEAR CASES OF THE APODIZED CHIRPED GRATING (SINE PROFILE)**

**TABLE 3**  
**THE MAXIMUM VALUES OF REFLECTIVITY,  $R_{\max}$ , FOR THE DIFFERENT PROFILES IN THE LINEAR AND NONLINEAR CASES AT 0 AND 1 KM.**

Profile	Linear Case $n_2 = 0 \text{ m}^2/\text{W}$		Nonlinear Case $n_2 = 2.6 \times 10^{-20} \text{ m}^2/\text{W}$	
	$R_{\max}$ at 0 km	$R_{\max}$ at 1 km	$R_{\max}$ at 0 km	$R_{\max}$ at 1 km
Blackman	0.92	0.935	0.96	0.975
Cauchy	0.91	0.92	0.95	0.965
Sinc	0.94	0.94	0.99	0.99
Sine	0.91	0.92	0.95	0.96
Tanh	0.87	0.88	0.9	0.91
Gauss	0.89	0.9	0.93	0.945
Hamming	0.85	0.865	0.88	0.89
Bartlett	0.88	0.89	0.91	0.92
Raised Sine	0.9	0.91	0.94	0.955

#### IV. CONCLUSION

The reflectivity of chirped FBG changes according to the apodization profile. A comparison between the different profiles leads to choose the best one in the wavelength selection performance. Sinc profile is the profile having the greatest reflectivity ( $R \approx 0.99$  in the nonlinear case), while the lowest one is in Hamming profile ( $R \approx 0.85$  in the nonlinear case) under the ocean depth effect. The obtained results show that the nonlinearity acts as a parameter that will help in the reflectivity increase by the increasing in the refractive index of the chirped FBG.

#### REFERENCES

- [1] K. O. Hill and G. Meltz, "Fiber Bragg Grating Technology: Fundamentals and Overview," J. Lightwave Technol., vol. 15, pp. 1263-1276, 1997.
- [2] K. Hinton, "Dispersion Compensation Using Apodized Bragg Fiber Gratings in Transmission," J. Lightwave Technol., vol. 16, pp. 2336-2346, 1998.
- [3] G. Lenz, B. J. Eggleton, C. R. Giles, C. K. Madsen and R. E. Slusher, "Dispersive Properties of Optical Filters for WDM Systems," IEEE J. Quantum Electron., vol. 34, pp.1390-1402, 1998.
- [4] F. Ouellette, "Limits of Chirped Pulse-Compression with an Unchirped Bragg Grating Filter," Appl. Opt., vol. 29, pp. 4826-4829, 1990.
- [5] B. J. Eggleton, T. Stephens, P. A. Krug, G. Dhosi, Z. Brodzeli and F. Ouellette, "Dispersion Compensation Using a Fiber Grating in Transmission," Electron. Lett., vol. 32, pp. 1610-1611, 1996.
- [6] Andreas Othonos and Kyriacos Kalli, Fiber Bragg Gratings, 2nd ed., Artech House, Norwood, 1999.
- [7] J. S. Aitchison, "Observation of Spatial Optical Solitons in a Nonlinear Glass Waveguide," Opt. Lett., vol. 15, pp.471-473, 1990.
- [8] Roger H. Dtolen, "Measurements of the Nonlinear Refractive Index Long Dispersions-Shifted Fibers," IEEE, J. Quantum Electron., vol. 16, No. 6, pp. 655-659, 1991.